GEOLOGICA CARPATHICA, AUGUST 2019, 70, 4, 279–297 doi: 10.2478/geoca-2019-0016

Turbidite sedimentology, biostratigraphy and paleoecology: A case study from the Oligocene Zuberec Fm. (Liptov Basin, Central Western Carpathians)

DUŠAN STAREK ✉, VLADIMÍR ŠIMO, SILVIA ANTOLÍKOVÁ and TOMÁŠ FUKSI

Earth Science Institute of the Slovak Academy of Sciences, Dúbravská cesta 9, 840 05 Bratislava, Slovakia; ✉dusan.starek@savba.sk

(Manuscript received December 17, 2018; accepted in revised form June 4, 2019)

Abstract: Outcrops of a thick turbiditic succession are exposed on the northern bank of the Liptovská Mara reservoir near Liptovská Ondrašová and Ráztoky. The section consists of rhythmic, predominantly thin- to medium-bedded turbidites of the Rupelian age. Their biostratigraphy is based on the calcareous nannofossils. Facies associations of these deposits represent different components of depositional lobe deposits in the turbidity fan system, including mainly the lobe fringe and lobe distal fringe/inter-lobe facies associations and locally the medium bedded deposits of the lobe off-axis facies association. This interpretation is supported by statistical analysis. The deep-sea turbiditic deposits contain trace fossil associations, which include deep-tier fodinichnia and domichnia up to shallow-tier graphoglyptids. Paleocurrent measurements indicate that the majority of sedimentary material was transported from SW and W.

Keywords: Western Carpathians, Oligocene, turbidites, trace fossils, calcareous nannofossils.

Introduction

The Oligocene sand-rich turbiditic system represents an important component of the Central Carpathian Paleogene Basin (CCPB). Turbidites form a large part of the Liptov Depression infilling, which is located in the northern part of the CCPB, but in contrast to the adjacent regions (e.g., Orava–Podhale or Spišská Magura), deposit outcrops are poor in the Liptov Depression and larger sedimentary profiles, suitable for sedimentological, biostratigraphic or paleoecological studies are scarce currently. We present the results of research on an unusual section of a turbidite series which is exposed on the banks of the Liptovská Mara Reservoir near Liptovská Ondrašová village (north-west edge of the Liptovský Mikuláš town) (Fig. 1C,D). This turbidite succession offers more than 700 completely exposed beds and provides a unique opportunity to study vertical variation in bed thickness and sedimentary structures. Occurrence of turbidite facies, their frequency and vertical relationships, the sandstone and mudstone ratio are important features used for discrimination of facies associations and interpretation of the depositional environment. Measurements of numerous paleocurrent indicators allowed determinations of the main paleotransport direction in this part of the basin. Detailed biostratigraphic analysis of calcareous nannofossils through the entire section allowed dating of these turbidite series. Paleoenvironmental evidence from study of trace fossils is beneficial within a section that lacks macro fossils. Only sporadic attention has been paid to trace fossils within the Liptov Depression of the CCPB (Plička 1983, 1984, 1987; Plička et al. 1990).

Geological settings

The CCPB lies inside the Western Carpathian Mountain chain (Fig. 1A) and belongs to the basinal system of the Peri- and Paratethyan seas. The CCPB opening and evolution is probably related to crustal thinning, either as a result of subcrustal erosion (e.g., Kázmér et al. 2003), or due to the extensional collapse of the overthickened Central Western Carpathian crust and the pull of the External Western Carpathian oceanic lithosphere retreating subduction (Plašienka & Soták 2015; Kováč et al. 2016).

The basin covered a large part of the Central Western Carpathian area (Fig. 1A,B) and is mainly filled up with marine, predominantly turbidite deposits which overlap the nappe units substrates and their thickness reach up to 1000 m. Their age ranges from the Bartonian (e.g., Samuel & Fusán 1992; Gross et al. 1993) to the Late Oligocene (cf. Olszewska & Wieczorek 1998; Gedl 2000; Soták et al. 2001, 2007; Garecka 2005). The CCPB sediments are preserved in many structural sub-basins (Fig. 1B), located in the Žilina, Rajec, Turiec, Orava, Podhale, Liptov, Poprad, and Hornád regions as well as in the Spišská Magura, Levočské vrchy and Šarišská vrchovina Mts.

The study area is a part of the Liptov Depression which is one of the largest inner-Carpathian depressions. The Liptov Depression is formed predominantly by the CCPB sediments overlain by Quaternary deposits of variable thickness. Paleogene deposits are bounded by the Mesozoic Central Carpathian units and their contact is transgressional in the south while the northern boundary is mostly tectonic (Fig. 1C).

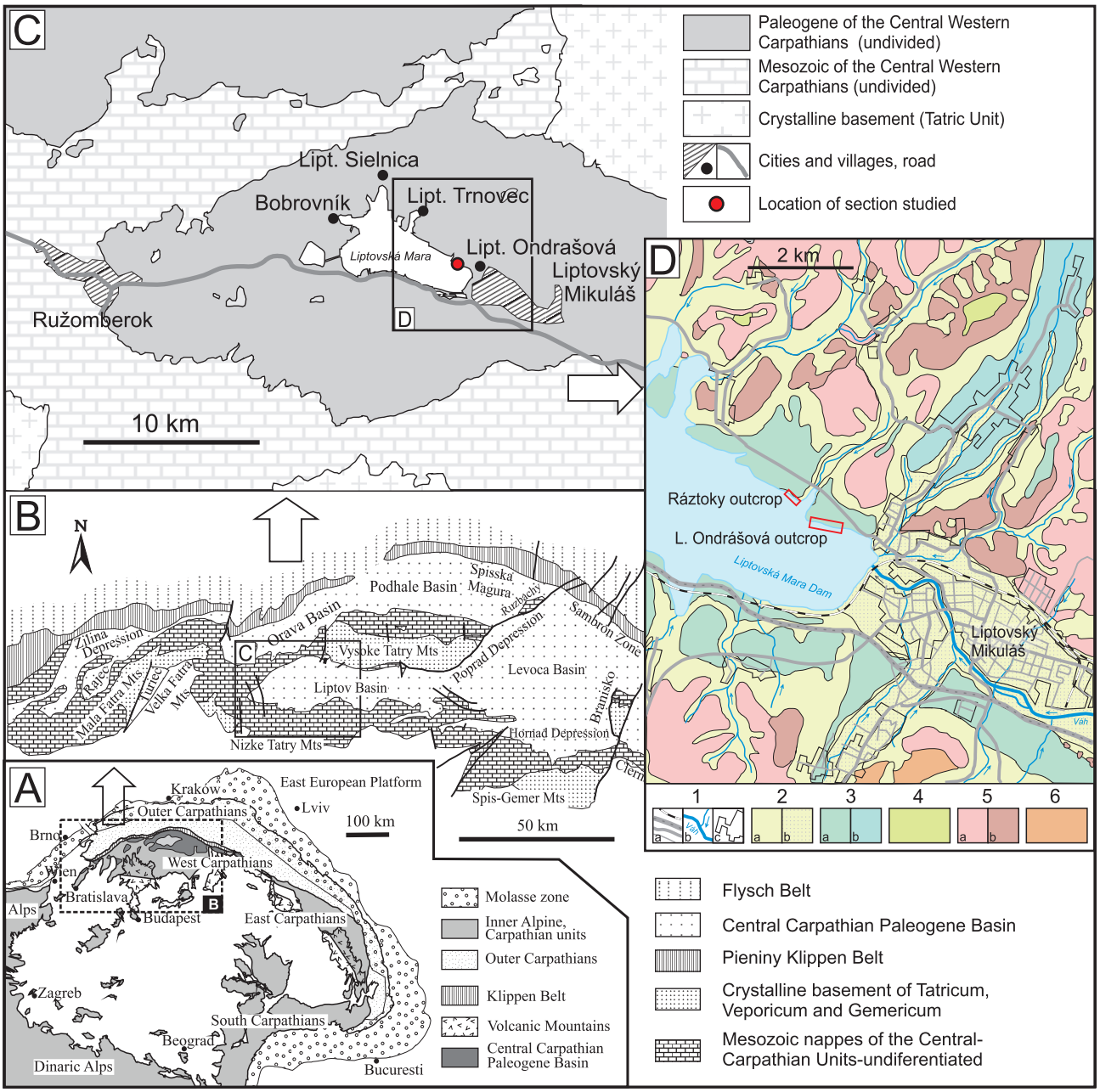

Fig. 1. **A** — Location of study area within the Alpine-Carpathian orogen; **B** — the Central Carpathian Paleogene Basin system depicting structural sub-basins, basement massifs and surrounding units; **C** — simplified geological sketch of the part of the Liptov region (after Biely et al. 1996; modified) with situated locality studied; **D** — situational geological map of the wider area of the studied localities (Geological Map of Slovakia M 1:50,000 [online] 2013); key: 1 — a) roads and railway, b) rivers, c) built-up area (cities and settlements); 2 — a) deluvial deposits, landslides (Quaternary), b) fluvial deposits (Holocene); 3 — a) fluvial and b) glaciofluvial gravels (Quaternary); 4 — Banská Bystrica Formation: sand, clayey sand, gravel (Neogene); 5 — Zuberec Formation: a) normal flysch: mudstones, siltstones and sandstones, b) flysch with predominance of mudstones and mudstone sequences in flysch deposits (Paleogene); 6 — Huty Formation: mudstones in absolute predominance over sandstones and conglomerates (Paleogene). Location of studied sections (Liptovská Ondrašová outcrop: 49°05'52.56" N, 19°34'22.98" E; Ráztoky outcrop: 49°06'06.02" N, 19°33'56.51" E).

The CCPB deposits (so-called the "Podtatranská skupina Group" *sensu* Gross et al. 1984; Gross 2008) are divided commonly into the following formations (Fig. 2) (Gross et al. 1984): the lowermost Borové Formation consists of breccias, conglomerates, lithic sandstones to siltstones, marlstones, organodetrital and organogenic limestones. These represent the basal terrestrial and shallow-marine transgressive deposits (e.g., Marshalko 1970; Kulka 1985; Gross et al. 1993; Baráth & Kováč 1995; Filo & Siráňová 1996, 1998; Šurka et al. 2012; Jach et al. 2016). This formation is overlain by the Huty Formation which includes various mud-rich deep marine deposits mainly (e.g., Janočko & Jacko 1999; Soták et al. 2001;

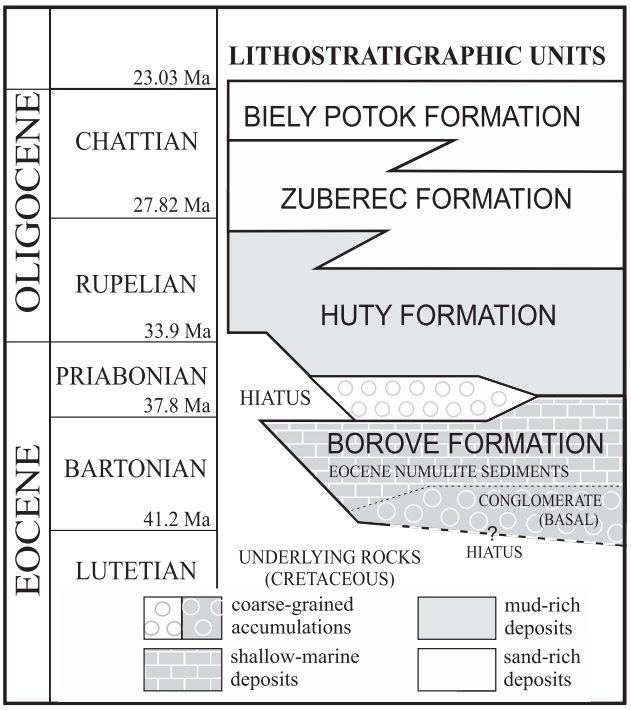

Fig. 2. Descriptive lithostratigraphy of the filling in the western part of the Central-Carpathian Paleogene Basin. Nomenclature of the formations according to Gross et al. (1984, adapted). Biostratigraphy is based on the data from Olszewska &Wieczorek (1998), Gedl (2000), Starek et al. (2000), Starek (2001), Garecka (2005) and Soták et al. (2007).

Starek et al. 2004) with the occurrences of sandstone megabed events (Golab 1959; Sliva 2005; Starek et al. 2013). The Zuberec Formation and the Biely Potok Formation compose the up-section, predominantly consisting of rhythmically bedded turbidites and massive sandstones and represent the various sand-rich submarine fan facies associations (e.g., Westwalewicz-Mogilska 1986; Wieczorek 1989; Soták 1998; Starek et al. 2000; Sliva 2005; Starek & Fuksi 2017a, b).

The evaluated and interpreted deposits are part of the Zuberec Formation (earlier known as "Flysch lithofacies" e.g., Gross et al. 1980) within which the above mentioned authors allocated several lithofacies with respect to the sandstone and mudstone proportions. They interpreted the age of this formation as the Priabonian–Lower Oligocene. The Oligocene age of the Zuberec Formation has also been confirmed in other parts of the CCPB (e.g., Olszewska & Wieczorek 1998; Gedl 2000; Soták et al. 2001; Garecka 2005; Filipek et al. 2017).

Methods

The research involved a standard sedimentological analysis of the sections. Bed thicknesses measurement and facies analysis were a key for further statistical analysis. Determination of the bed thickness becomes complicated if it is thinning out laterally, contains preserved bedform morphology or the bed has an uneven — erosive base. In these cases the average thicknesses were used.

Paleocurrent analysis included scour mark measurements and current ripple cross-laminations. Postdepositional tilt of the directions was restored by simple rotation along the horizontal axis.

Calcareous nannofossils

Thirty-nine samples were evaluated to study calcareous nannofossils from the Liptovská Ondrašová locality. Six samples come from a non-profiled part of outcrop. Samples for the calcareous nannofossils study were prepared from mudstones containing $CaCO_3$ by using the decantation method (Haq & Lohmann 1976; Perch-Nielsen 1985). The smear slides were studied under the light microscope ZEISS AXIO SCOPE AI, at 1000× magnification and nannofossil species documented by digital camera AXIOCAM 105 COLOR. Calcareous nannofossil age determination was carried out according to the zonation by Martini (1971), supplemented by Perch-Nielsen (1985), Young (1998) and Nannotax websites (Young et al. 2017). Preservation and abundance of calcareous nannofossils was determined according to Roth & Thierstein (1972).

Statistical analysis

Sandstone and mudstone thickness were used for statistical analysis. Specifically, 725 beds from 2 profiles (Liptovská Ondrašová 1=566; Liptovská Ondrašová 2=159 beds), in total length of more than 77 m (unlike the total length of outcrop 92 m) could be measured. All beds were measured in step by 0.5 cm. No correction was made for compaction. Sandstone–mudstone ratio, mean, median, minimum, maximum and standard deviation of sandstone and mudstone thickness were used to identify differences between profiles. Boxplot and histogram functions demonstrated variability within profiles and expressed the frequency distribution of bed thicknesses. Autocorrelation or serial correlation is a tool for identifying repeating patterns (Priestley 1981). Autocorrelation shows correlation between the lagged values of the time series. It can be interpreted as periodicity. The autocorrelation coefficient values close to zero show no periodicity (Pinheiro et al. 2018). Coarse-division (sandstone) thicknesses of turbidite beds were processed by Hurst statistics. Hurst exponent is related to autocorrelation of series (Hurst 1951, 1956; Chen & Hiscott 1999). Recalculated K and D values from Hurst statistics can be used to depositional environment interpretation (Chen & Hiscott 1999). Coarse-division (sandstone) thicknesses were used for computation of cumulative distribution also. Typically, this function shows a degree of variation from the power-law (straight-line) distribution and is calculated and examined on a log plot. 2D model simulates proximal vs. distal (non-channelized) environment effect (Carlson & Grotzinger 2001). All analyses were processed by R-cran software (R Core Team 2014) and package *nlme* (Pinheiro et al. 2018).

Description of outcrops

The outcrop studied near Liptovská Ondrašová shows a long succession in which two continuously exposed sections Liptovská Ondrašová 1 (LO1) and Liptovská Ondrašová 2 (LO2) were processed (Fig. 3A). LO1 has a total length of more than 68 m and LO2 is more than 23 m long. Within the studied profiles the sedimentary successions show relatively monotonous lithology of alternating sandstones and mudstones. Between LO1 and LO2 sections there is an uncovered or poorly outcropped part about 10–15 m long. Here the shorter, non-continuously exposed portions indicate mudstone and mainly thin-bedded sequences. However, because of this relatively large interruption of the sedimentary sequence, we have processed and evaluated the obtained dataset as two separate parts (LO1 and LO2). The LO2 section ends at a pier on the edge of the Ráztoky Bay. Further exposures appear on the shore of the lake, on the other side of the bay, towards the cadastral area of the Ráztoky village drowned by damming (Fig. 1D). The following will be referred as the Ráztoky locality. The exposed sedimentary sequences at the Ráztoky locality are tectonically fractured and are not suitable for detailed profiling.

Results

Sedimentary facies

Since the sedimentary facies within the LO1 and LO2 sections with the Ráztoky locality as well, are very similar, they are described together in the following description. This classification is based on lithology and primary sedimentary structures mostly. The following sedimentary facies were identified: unstructured ungraded to normally graded medium- to fine-grained sandstone; parallel-laminated medium- to fine-grained sandstone; sandstone with asymmetrical cross-lamination; coarse-grained to fine-grained laminated siltstone; massive mudstone and mudstone, parts of which reveal an increased content of silt and very fine sand (graded and laminated mudstone). Sedimentary facies identified within deposits of individual sections reflect deposition from sandy high- to low density turbidity current (Bouma 1962; Mutti 1992). More detailed hydrodynamic interpretation of individual facies as well as possible identification of the same facies from other authors is shown in Table 1. However, in the following text the Bouma classification (Ta–Te divisions sensu Bouma 1962) is used for better clarity of identified sedimentary facies.

Table 1: Sedimentary facies and their interpretation within the studied sections.

Facies	Interpretation
Unstructured ungraded to normally graded medium- to fine-grained sandstone (Fig. 4A)	A rapid accumulation of sand from dense sandy turbidity current which bypassing the zone of deposition of the preceding gravelly flows — Ta division (sensu Bouma 1962) or F8 facies (after Mutti 1992)
Parallel-laminated medium- to fine-grained sandstone (Fig. 4A–D)	The upper flow regime conditions; traction carpet that is driven by basal shearing of an overlying turbulent flow — Tb division (sensu Bouma 1962) or F9 facies (after Mutti 1992)
Sandstone with asymmetrical cross-lamination (Fig. 4E,F)	The lower flow regime; traction movement with fallout processes from waning turbidity currents (e.g., Jopling & Walker 1968; Mulder & Alexander 2001; Zavala et al. 2011) — Tc division (sensu Bouma 1962), F9 facies (after Mutti 1992)
Coarse-grained to fine-grained laminated siltstone	Traction plus fallout processes associated with deposition from suspension during weak turbulent motion in low-density turbidity currents (Arthur et al. 1984; Stow & Piper 1984) — Tb division (sensu Bouma 1962), E1 interval (after Piper 1978) or F9 facies (after Mutti 1992)
Massive mudstone, some parts reveal an increased contents of silt and very fine sand (graded and laminated mudstone) (Fig. 4G)	Suspension fall-out from static or slow-moving mud cloud; flnal deposition from a sediment gravity flow event (e.g., Piper 1978) — Te division (sensu Bouma 1962), T6 and T7 divisions (after Stow & Shanmugam 1980 — graded and ungraded turbidite muds respectively)

Fig. 3. A — Sedimentary logs of rhythmical bedded, sand/mud-mixed turbidite succession of the Zuberec Fm. studied in an outcrop near Liptovská Ondrášová. The chard depicts vertical distribution of sandstone- and mudstone thicknesses and their possible trends, the sedimentary facies, the facies associations, and sampling for stratigraphy. **B** — Schematic model for the facies associations of the Liptovská Ondrášová sections. Individual facies associations represent different components of distributive lobe deposits (model after Prelát et al. 2009, modified). **C** — LO2 section; note the gradual transition between mudstone dominated sequence (FA4) in the bottom of the outcrop and rhythmically bedded sandstone-mudstone sequence (FA3) towards the top of the profile. **D** — Thinning-upward trend of sandstone bed thickness from medium- to thick beds with smaller ratio of mudstones (FA2) in the lower part of the picture to thin bedded sequence FA3 in middle part and mudstone dominated FA4 in the upper part of the picture. **E** – Turbidite sequence characterized by FA3 and FA2. Thickening-upward trend of sandstone beds is highlighted by white arrow. Note the erosive character of some beds in Fig. 3D,E (highlighted with small black arrows). **F** — Rhythmically bedded turbidite sequences with relatively balanced sandstone–mudstone ratio in the middle and top of the outcrop (FA3). The lowermost part of the outcrop with mudstone dominated unit corresponds to FA4. Note the relatively sharp transition between thin-bedded part and medium-bedded upper part of succession. **G** — detailed view of very regular thin-bedded, mudstone dominated sequences typical for lobe distal fringe/inter-lobe environment (FA4). The scale corresponds to 10 cm.

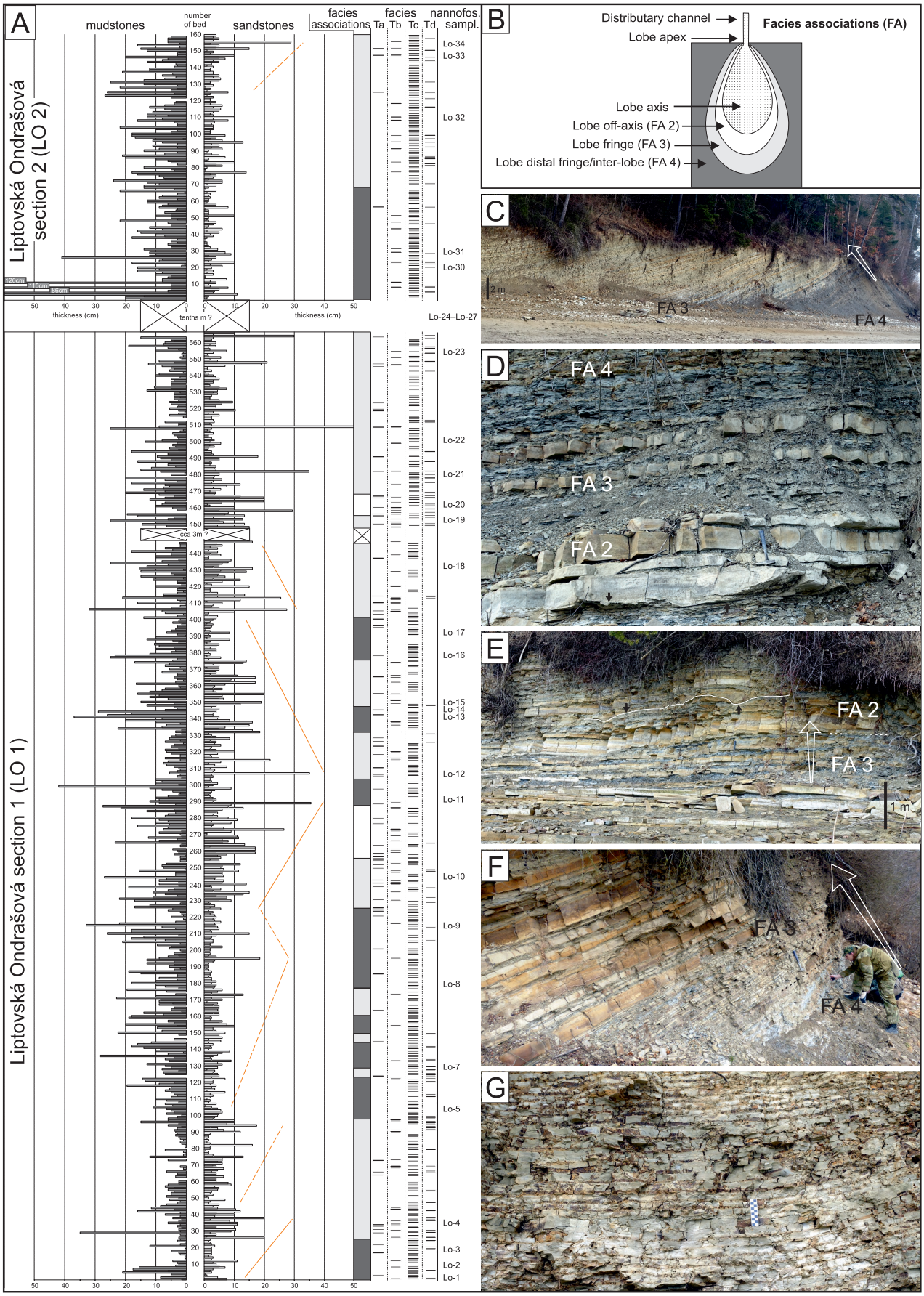
A
mudstones
number of bed
sandstones
facies associations
facies Ta Tb Tc Td
nannofos. sampl.
Liptovská Ondrašová section 2 (LO 2)
Liptovská Ondrašová section 1 (LO 1)
thickness (cm)
tenths m ?
cca 3m ?
Lo-34
Lo-33
Lo-32
Lo-31
Lo-30
Lo-24–Lo-27
Lo-23
Lo-22
Lo-21
Lo-20
Lo-19
Lo-18
Lo-17
Lo-16
Lo-15
Lo-14
Lo-13
Lo-12
Lo-11
Lo-10
Lo-9
Lo-8
Lo-7
Lo-5
Lo-4
Lo-3
Lo-2
Lo-1
B
Distributary channel
Lobe apex
Facies associations (FA)
Lobe axis
Lobe off-axis (FA 2)
Lobe fringe (FA 3)
Lobe distal fringe/inter-lobe (FA 4)
C
2 m
FA 3
FA 4
D
FA 4
FA 3
FA 2
E
FA 2
FA 3
1 m
F
FA 3
FA 4
G

Apart from minor exceptions, the whole evaluated sedimentary succession comprises beds which are composed of medium- to very fine-grained sandstone with a typical vertical arrangement of divisions Ta, Tb and Tc. Here continuous transition to Td and Te divisions is common. Generally, the Ta division usually forms the gradational interval in the turbidite lowermost part, especially on thicker beds. Not all beds have developed complete Ta–Te Bouma divisions (Fig. 4A). The beds (especially thicker ones) are often characterized only by Ta and Tb divisions with a rapid transition into siltstones and mudstones (Td, Te). The lower bed interfaces are sharp and plain mostly, rarely gently undulated (loading deformation). Some beds show complex internal arrangement of individual facies and they multiply repetitions within a single bed (Fig. 4B,C). This type of complex bedding shows a symmetrical arrangement of divisions (Tb–Ta–Tb) (Fig. 4D). On the contrary, most of the thin beds (up to 3–5 cm) have developed the ripple lamination only (Tc). These beds often show completely preserved bedform morphology (Fig. 4E, F). Mudstones are layered with very thin laminae (in mm scale) of siltstone and/or very fine-grained sandstone frequently. They are fine horizontally laminated or small scale ripple laminated with completely preserved bedform morphology (Fig. 4G). Some ripple laminated beds show pinching out character, especially the thinner of them. In very rare cases, the beds erosive character may be observed with development of shallow scour structures as well (Fig. 4H,I). The erosive character of some currents indicates the presence of floating mudstone intraclasts (Fig. 5A) which are rarely embraced on the top of the sandstone bed. The base of the beds is characterized by relatively common small-size erosional current marks (Fig. 5B–D) and trace fossils (*see* Ichnofossils chapter). Loading and dilatation ridges are much rarer (Fig. 5E), as well as coalified phytodetritus on separated bedding planes (Fig. 5F).

Facies associations

Within the studied sections, in the sense Prélat et al. (2009), the distinguished facies associations mostly correspond to the lobe fringe and lobe distal fringe/inter-lobe facies associations and to a small extent also lobe off-axis facies association (Fig. 3B). For easier comparison we denote the related facies associations as FA2–FA4 (identically as So et al. 2013). The facies association corresponding to the lobe axis (FA1) cannot be identified therefore, the following description begins with FA2.

Locally occurring sequences from the middle to upper part of the LO1 section (Fig. 3A) may represent lobe off-axis facies association (FA2). They are represented by medium-thick sandstone beds and balanced to slightly predominant ratio of sandstones. (Fig. 3D,E). In thicker sandstone beds (>15 cm), massive bedding is the most common (ungraded to normally graded sandstone — Ta division). The Ta division within thick beds is commonly overlain by parallel-laminated sandstones (Tb division) or may fining upwards with relatively sharp transition to siltstone and mudstone facies. The ripple cross-lamination (Tc division) is rather sparse in thick sandstone beds and is poorly developed. They form only thin intervals at the top of the beds, near the transitions to siltstones. The geometry of each bed is tabular or sheet-like and generally the beds have a good lateral stability. Especially within this facies association, beds occur with complex internal arrangement of individual facies in which multiple repetition is frequent (Fig. 4B–D), apart from the more frequent Ta division and rare occurrence of shallow scour structures (Fig. 3D,E).

The medium- to fine grain sizes of most sandstones, tabular geometry of beds, occurrence of medium-bedded sandstone with massive bedding, intercalation of thin- bedded turbidites with abundant Tb, Tc, and Td divisions as well as absence of both — some metres to tens metres thick bedseds of massive, frequently amalgamated thick sandstones, and large scours or evidence for channels suggest deposition in the lobe off-axis environment (Prélat et al. 2009; Prélat & Hodgson 2013; So et al. 2013).

In lobe fringe facies association (FA3) mudstone beds are predominant (60–70 %). The main component of this facies is rhythmic thin-bedded sequence with sandstone and mudstone beds, generally ranged from several cm to tens cm in thickness (Fig. 3C–F). Beds are tabular or sheet-like and generally they have a good lateral stability. The lower bed interfaces are sharp with common small-size erosional current marks (Fig. 5B–C). Lobe fringe facies association comprises all identified sedimentary facies and the beds often show complete developed Bouma divisions (Ta–Te, sensu Bouma 1962). However, unstructured ungraded- to normally graded sandstone facies is much rarer compared to others (Tb–Te divisions) and usually builds the rare thicker beds (up to 15–20 cm) or lowermost part of the thiner turbidites. The Ta division is less common as in the FA2. Especially thin, very fine-grained, up to 5 cm thick turbidites consist of Tc–Te divisions only.

A regularly thin-bedded, rhytmic, some metres thick sequence with a high proportion of mudstone, thin-bedded finely-structured sandstone with good lateral continuity supported interpretation of FA3 as lobe fringe deposits (Prélat & Hodgson 2013; So et al. 2013).

Lobe distal fringe/inter-lobe facies association (FA4) is dominated by thin-bedded fine to very fine-grained sandstones, siltstones, and medium- to thick-bedded mudstones mainly. In this facies association, mudstones have a strong dominance and often make up more than 70 % of the total thickness of FA4. Tc–Te divisions are frequent, but the sandstone Ta and Tb divisions are very sporadic. This facies association forms shorter sequences in the whole sections but reaches its maximum thickness in the lowermost part of LO2 where the mudstone thickness forms up to 120 cm (Fig. 3A). A large part of the poorly uncovered succession between LO1 and LO2 sections as well as succession at the Ráztoky locality probably also belong to this facies association. Regularly thin-bedded, fine- to very fine-grained turbidites with good lateral continuity and height contents of

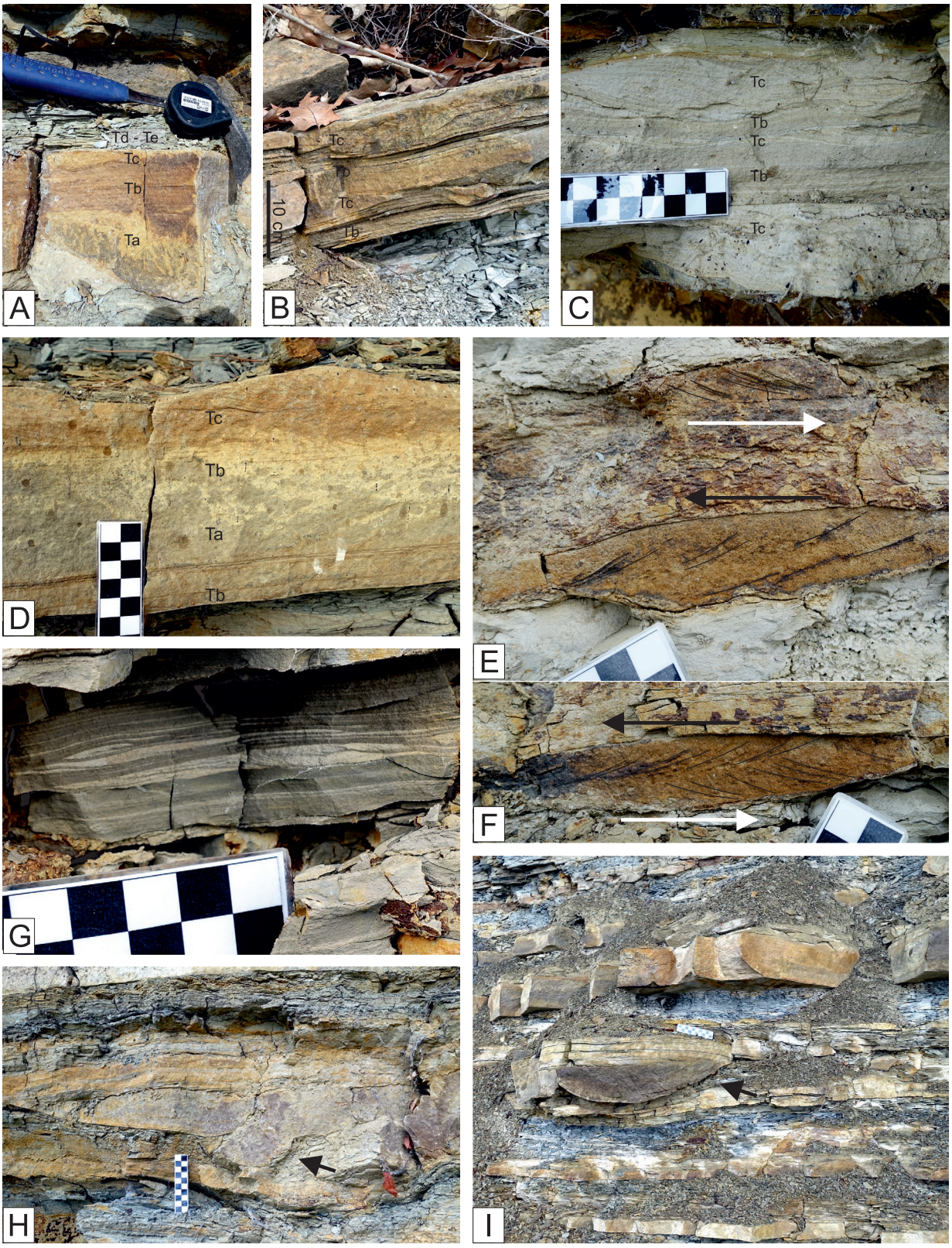

Fig. 4. Sedimentary facies and structures. **A** — Lithological couple formed by fine-grained sandstone and mudstone with complete "Bouma sequence" (Ta–Te divisions); **B, C** — complex internal arrangement of bed with multiple repetition of individual facies within a bed; **D** — symmetrical arrangement of facies in sandstone bed; **E, F** — ripple cross-laminated sandstone beds with completely preserved bedform morphology. Note the oppositely oriented lamination within separate beds (E) as well as herringbone structure in a single bed (F); **G** — mudstone with fine lamination of very fine-grained sandstone to siltstone; **H, I** — small-scale erosive scours (black arrows). A black field on the scale corresponds to 1 cm.

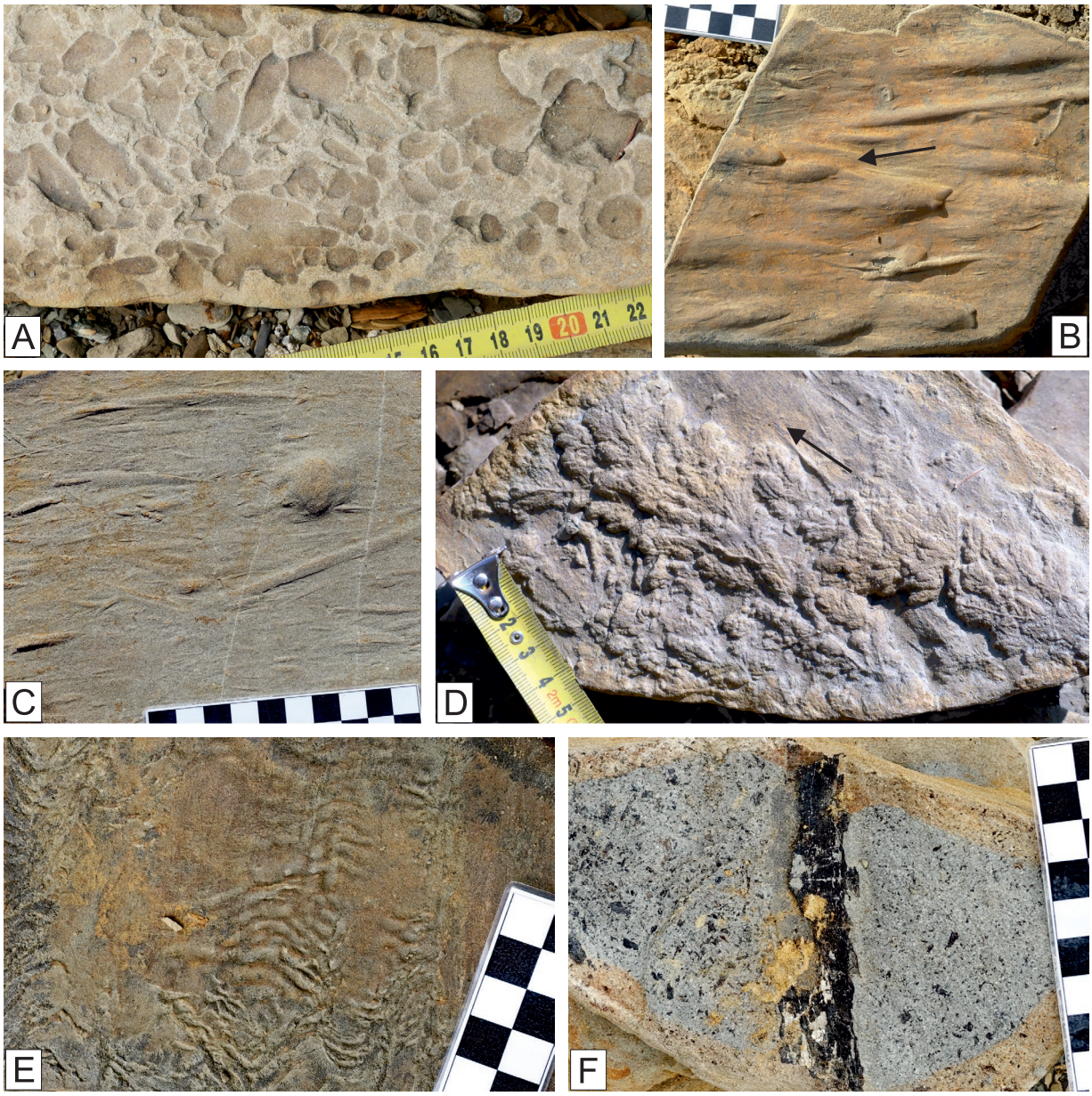

Fig. 5. Structures on bedding planes. **A** — Sandstone molds of weathered mudstone intraclasts; **B** — flute casts; **C** — small scale of tool marks, a non-defined circular structure in the upper right part of the figure is probably of mechanical origin, similar to the impact or impress structure; **D** — frondescent marks (black arrows on the pictures indicate the direction of paleoflows); **E** — loading and dilatation ridges on the lower bedding plane; **F** — coalified plant detritus in sandstone. A black field on the scale corresponds to 1 cm.

mudstone facies support interpretation of FA4 as lobe distal fringe and inter-lobe with the deposition of dilute low concentration turbidity currents or slow hemipelagic deposition (Stow & Piper 1984).

Paleocurrent analysis

The typical features of the thin- to medium-bedded, fine-grained turbidity sequences are paleocurrent indicators such as oriented erosive structures on the bed soles (e.g., frondescent marks, flute marks, longitudinal furrows, ridges and tool marks (Fig. 5B–D) and current ripple cross-lamination. Paleocurrent data derived from the lower bedding plane structures, provide general flow orientation SW–NE with transport in a NE direction (Fig. 6). These indicators show relatively small variation and orientation remains constant throughout the whole studied section. Paleocurrent data derived from ripples shows a more significant variability with transport in a SE–NE direction. Rarely, some current ripples show measurements of contra-directional orientation with transport NW direction. These contradictory ripple laminations occur within separate beds (Fig. 4E) or oppositely oriented parts of laminations within cross-bedded layers where herringbone cross-stratification has formed (Fig. 4F).

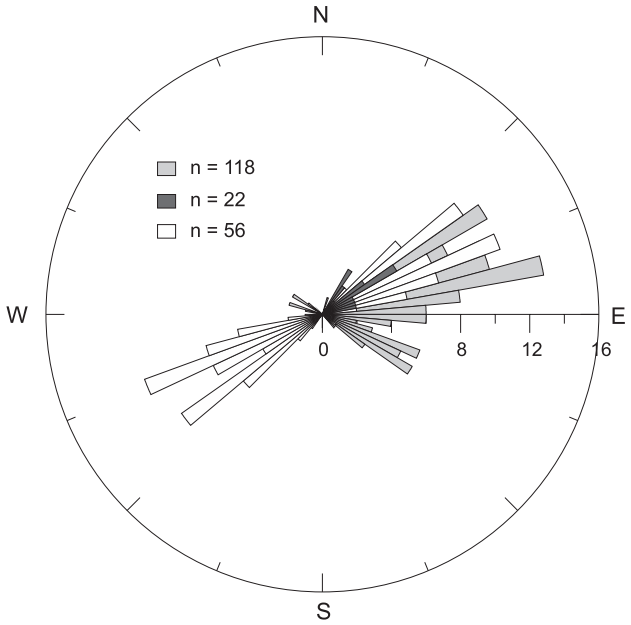

Fig. 6. Paleocurrent data derived from oriented erosive structures on the lower sides of the beds (white: orientations, dark-grey: directions) and current ripple cross-lamination (light-grey).

Bed thickness statistical analysis

The sections consist of rhythmic, predominantly thin- to medium-bedded successions which differ mainly by ratio of sandstone (LO1: 44.5 %, LO2: 24.2 %) and mudstone beds (LO1: 55.5 %, LO2: 75.8 %). The vertical arrangement of all beds from both sections, as well as the variability in sandstone–mudstone proportion, is depicted in Fig. 3.

Beds have variable thickness up to 50 cm (Figs. 3A, 7A). Only a few mudstone beds reach greater thicknesses (60–120 cm) in the lowermost part of the LO2 section.

Boxplots and histograms show thickness distributions (both sandstone and mudstone divisions) of the beds among individual profiles (Fig. 7A,B). The average thicknesses of turbidite sandstone facies are 5.4 cm (LO1 section) and 3.6 cm (LO2 section). In the LO1 section sandstone beds with thicknesses smaller than 5 cm are most frequent. 50 % of the beds range between 2 and 6 cm. Mudstones from this profile are represented mostly by beds thinner than 6 cm. In contrast, the LO2 section is characterized by thin rhythmically repeating sandstone beds of which 50 % are between 1.5 to 5 cm. Mudstone variability is higher here and 50 % of mudstone thicknesses range between 4 and 14 cm. Frequency distributions are right skewed and show higher proportions of small beds and beds thicker than 10 or 15 cm are rare.

Generally, beds show noncyclic vertical organization or only low-expressive vertical organization into small-scale series with upward thickening of sandstone beds. Bed thinning tendency is less common. Autocorrelation of coarse grained divisions also shows relatively weak periodicity on 16th, 18th and 27th beds in LO1 section and on every 4th bed in LO2 section (Fig. 7C). Other bed periodicity signals are insignificant. However, vertical patterns in bed arrangement of some few metres thick units show a clear upward thickening tendency (Fig. 3E,F).

The cumulative distribution of the complete coarse-division thicknesses from both profiles has an almost linear shape (Fig. 7D). Cumulative distributions on logarithmic scales y and x axes correspond to frequent occurrence of well defined thin turbidites in succession (Fig. 3A). Rare occurrence of a few thicker beds within the profile affects the line and bends its upper part slightly.

The Hurst coefficient was used to verify assumed interpretations of the depositional paleoe-nvironment (Chen & Hiscott 1999). The K (0.69–0.73) and D (1.9–3.8) values of coarse division thicknesses and their percentage within the Liptovská Ondrašová sections are located in a narrow field near the interface of basin-floor sheet sand and lobe-interlobe deposits (Fig. 7E).

Ichnofossils

Trace fossils found in the outcrops studied belong to 11 ichnospecies.

Arenicolites Salter, 1857
Arenicolites isp. (Fig. 8)

Arenicolites isp. was observed as a vertically oriented U-shaped burrow without wall. Pairs of openings on the bedding planes have the same diameters, but it also has sparsely dimorphic morphology. Diameters of sectioned burrows attain 2.5 to 3.7 mm. Depth of U-shaped burrows is up to 13 mm. Distances between pair opening vary between 7 to 14 mm. Burrow is relatively shallow. Arms of U-shaped burrow are not parallel but are slightly divergent. *Arenicolites* and *Saerichnites* burrows have the same range of diameters, which may imply that *Arenicolites* represents initial form of *Saerichnites* burrow system. This trace fossil belongs to domichnion, producer is thought to be suspension and/or deposits feeder polychaetes (Bromley 1996) and amphipod crustaceans (Baucon et al. 2014) in marine environment.

Arthrophycus Hall, 1852
Arthrophycus cf. *tenuis* (Książkiewicz, 1977) (Fig. 9A)

A. cf. *tenuis* was observed as hypichnial tiny sickle-shaped burrows with the tapered ends. Branching to bunch-shaped burrows were rare. The most typical forms of this ichnogenus are arranged into bundles but it is not typical of *A.* cf. *tenuis* at this locality. The trace fossil occurs on sole of bedding plane with occasionally occurrence of bioglyphes striae, which are oriented transverse through the trace fossil (modified according to Uchman 1998). *A.* cf *tenuis* has relatively high abundance in the lower part of described succession at the locality Liptovská Ondrašová. *Arthrophycus* is considered to be feeding burrows of arthropods and polychaetes (Seilacher 2007).

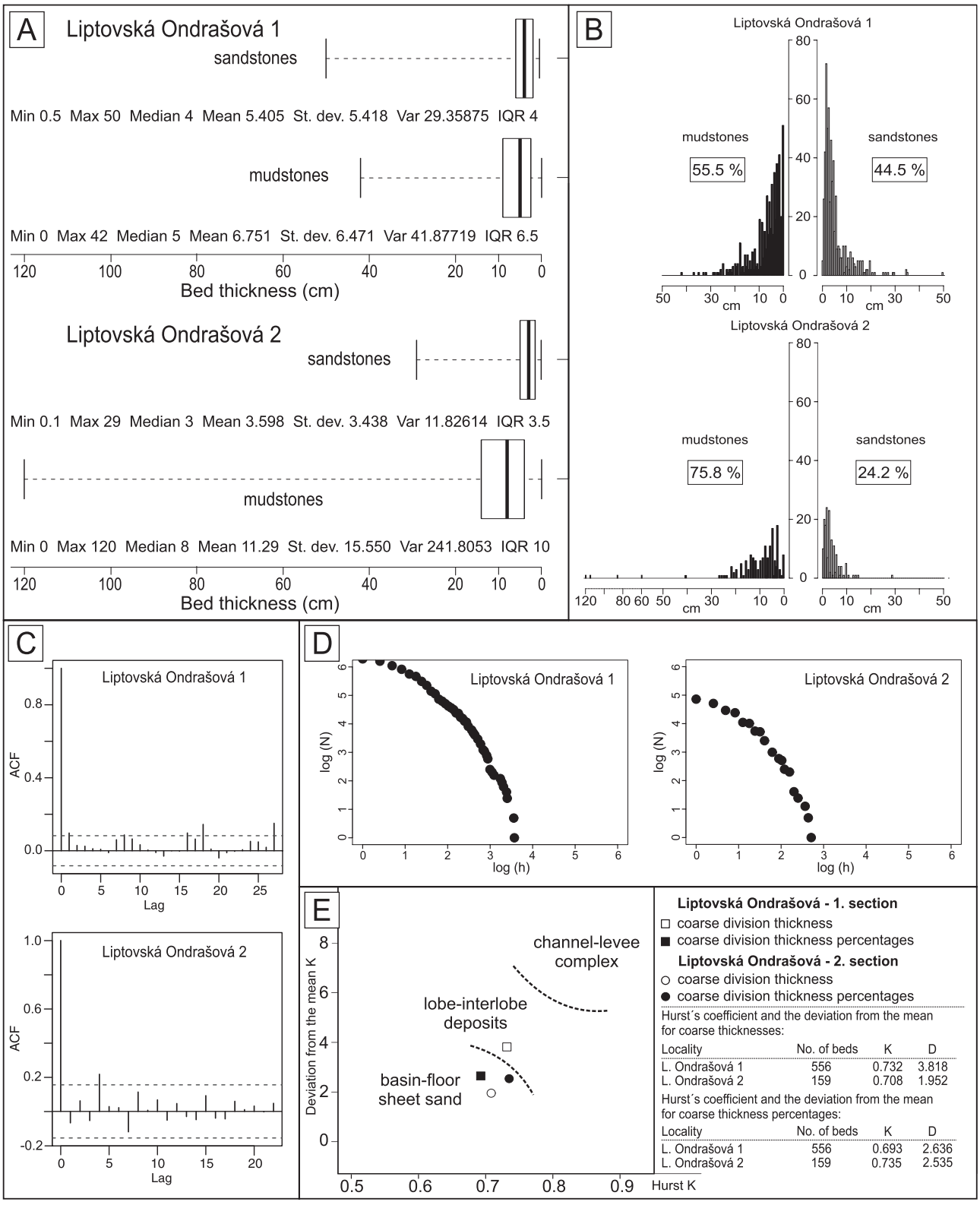

Fig. 7. Results of statistical analysis. **A** — Sandstone and mudstone division-thicknesses frequency distribution among individual sections; **B** — frequency analysis of sandstone as well as mudstone bed thicknesses within individual sections; **C** — time series analysis shows relatively weak periodicity within both sections. ACF — autocorrelation, Lag — the time lags; **D** — cumulative distribution of the sandstone thicknesses. The shape of line of cumulative distribution best corresponds with outer fan environment (cf. Carlson & Grotzinger 2001). **E** — Plot of Hurst K of an original succession against the deviation from mean K of the shuffled succession of individual sections (modified on the basis of the plot of Chen & Hiscott 1999).

Bergaueria Prantl, 1947
Bergaueria hemispherica Crimes et al. 1977 (Fig. 9B)

B. hemispherica is presented as a hypichnial knobby hemispherical symmetrical to slightly asymmetrical trace fossil without central depression. Height of observed *Bergaueria* attains 14 mm and its diameter is up to 36 mm. *B. hemispherica* surface is smooth, occasionally concentric patterns probably reflected boundaries of surrounding layers of mud or sandstone. Producers of *Bergaueria* are thought to be sea anemones (Bromley 1996).

Helminthopsis Heer, 1877
Helminthopsis tenuis Książkiewicz, 1968 (Fig. 9C)

Helminthopsis tenuis was observed as unbranched relatively long hypichnial, horizontal, cylindrical, wide, shallow, meander, 1 mm thick. This trace fossil occurs in shallow-marine to deep-sea facies, commonly in turbiditic deposits. Systematic revision of this ichnogenera (Wetzel & Bromley 1996; Uchman 1998) shows relatively wide variability within several ichnospecies. Producer of *Helminthopsis* probably belongs to polychaetes or priapulids (Fillion & Pickeril 1990). *H. tenuis* is relatively rare and it has been found at the Liptovská Ondrašová locality only.

Laevicyclus Quenstedt 1881
Laevicyclus isp. (Fig. 9D)

Only one specimen of this structure has been found on the sole bed. Provisionally without further samples it was assigned to *Laevicyclus* isp. It is consisted of two concentric circles. Outer circle attains diameter 6 mm and inner circle has 2.5 mm. Width of the circle strings is 0.3 mm. Central knob 0.9 mm in diameter with short string is situated inside the inner circle. However circular structures can be reflected *Bathysiphon* test scratch marks circular-shape mechanoglyphes also (Uchman & Rattazzi 2013).

Paleodictyon Meneghini 1850
Paleodictyon minimum Sacco 1888 (Fig. 9E)

P. minimum is typical of tiny mesh size that attains 2–2.2 mm. Measured string diameters are in the range 0.47 to 0.56 mm. A poorly preserved fragment of one specimen was found on the sole bed. Structure of ichnogenus *Paleodictyon* is characterized as shafts which run up from the middle of tunnels between the corners or from the point of corners of horizontally oriented hexagonal mesh to the sea bottom (Rona et al. 2009, fig. 8; Seilacher 2007, plate 55). *Paleodictyon* ichnotaxonomical summary revision has been provided by Uchman (1995).

Planolites Nicholson 1873
Planolites montanus Richter 1937 (Fig. 9F)

Planolites occurs as simple not branched burrows with smooth surface which are elliptical or circular in cross section. Diameter of observed burrows attains 0.9 to 1.2 mm and 30 mm length. This morphologically simple burrow is typical of cross-facies trace fossils (Fillion & Pickeril 1990).

Saerichnites Billings 1866
Saerichnites isp. (Fig. 9G,H)

This trace fossil has frequently been found on the upper bed surface as a view of sections of two rows of circular or semicircular weathered pits or positively weathered vertical or oblique burrows. Diameter of sectioned burrows arranged in the rows and it attain 2.4 to 3.2 mm in diameter. Morphology of such sectioned burrow can be interpreted by two ways: (i) horizontal burrow with branched shaft, or (ii) horizontally spiralled burrow (Uchman 1995, 1998; Fürsich et al. 2006).

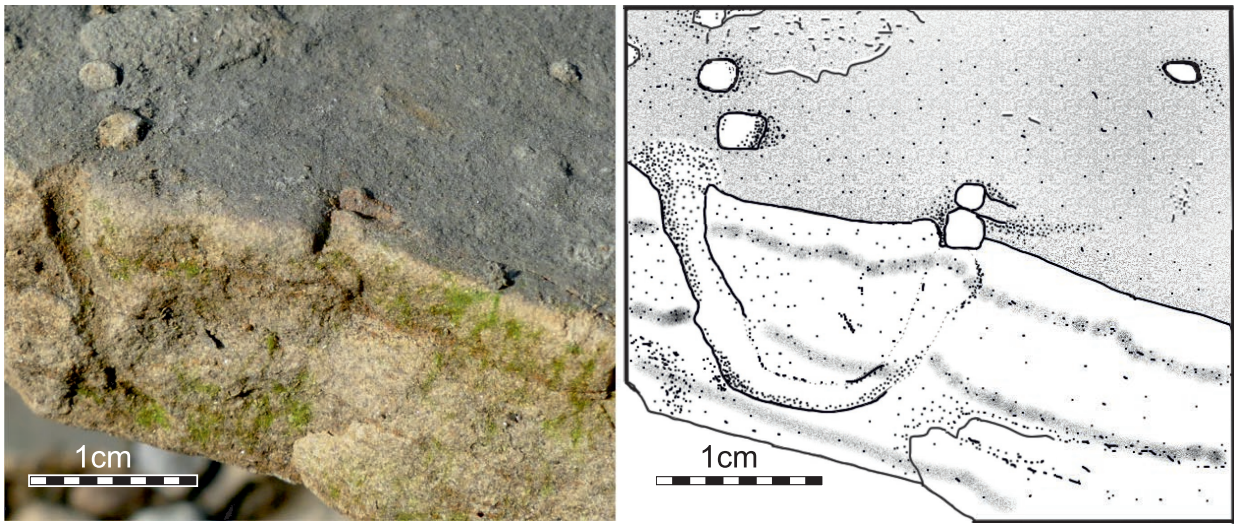

Fig. 8. *Arenicolites* isp. from the Ráztoky locality. Perpendicular section with weathered U-shaped burrow of *Arenicolites* isp. Several sectioned burrows on the bedding surface are visible.


A
1cm
B
1cm
1cm
G
1cm
C
1cm
D
0.5 cm
E
1cm
F
1cm
H
1cm
I
1cm
K
1cm
J
1cm
0.5 cm
L
1cm

Fig. 9. Trace fossil assemblage of the Liptovská Ondrašová and the Ráztoky localites. **A** — Sole bed with tiny scratchy like hypichnial lines of *Arthrophycus tenuis* (L. Ondrašová); **B** — *Bergaueria hemispherica* presents natural casts of biologically originated depressions that are situated on the sole beds. Upper and side views (Ráztoky); **C** — slim (up to 1 mm in diameter) unbranched irregularly meandered *Helminthopsis tenuis* occurs as a hyporelief (L. Ondrašová); **D** — rarely occurring hypichnial questionable specimen of *Laevicyclus* isp., this structure can be interpreted as scratch circle-shaped marks also (*sensu* Uchman and Rattazzi, 2013), (Ráztoky); **E** — poorly preserved *Paleodictyon minimum* on sole bed (Ráztoky); **F** — hypichnial, unbranched *Planolites montanus* is pointed by arrows. Trace in the right corner of the picture belongs to *Thalassinoides* (L. Ondrašová); **G, H** — vertical to subvertical oriented burrows arranged in the double rows of *Saerichnites* isp. on upper bedding surface (Ráztoky); **I** — hypichnial *Scolicia strozzii* double line traces produced by irregular sea urchins (L. Ondrašová); **J** — branched hypichnial burrow of *Strobilorhaphe clavata* with magnified part of triangular shaped tiny chambers (Ráztoky); **K** — *Thalassinoides suevicus* with Y-shaped branched burrows, swollen in area of branching, sole bed (L. Ondrašová); **L** — regularly meandered hypichnial fragmented trace fossil rare occurs on the Ráztoky locality.

This form of traces can be assigned into pearl string traces like *Hormosiroidea*, *Margaritichnus*, *Nereites*, *Parahaentzschelinia* and *Ctenopholeus* (Uchman 1995; Fürsich et al. 2006).

Scolicia De Quatrefages 1849
Scolicia strozzii (Savi & Meneghini 1850) (Fig. 9I)

At Liptovská Ondrašová relatively frequented trace fossils occurring on sole beds. It has double parallel ridge morphology. Diameter of specimen is in the range 12 to 20 mm. Diameter of the lobes is 3 to 6 mm. Lobes of ridges are semi-circular in cross-section. Meandering, diameter of trace fossil and lobe is often changing in the same specimen (Uchman 1995). Abundance of *S. strozzii* is low but it occurs on the Liptovská Ondrašová and Ráztoky localities. *Scolicia* is produced by irregular echinoids with double drainage tube assigned to the *Spatangus* group (Uchman 1995; Gibert & Goldring 2008).

Strobilorhaphe Książkiewicz, 1968
Strobilorhaphe clavata Książkiewicz, 1968 (Fig. 9J)

Strobilorhaphe clavata has hypichnial branched burrow with numerous laterally arranged cone shaped chambers. Length of the chamber attains 7.2 mm and the width is from 3 to 3.3 mm. Diameter of the burrow is unclear because it is covered by lateral clavate chambers. Książkiewicz (1977) noted that the burrow is 2 mm wide. Common abundance of *S. clavata* is registered only at the locality Ráztoky.

Thalassinoides Ehrenberg 1944
Thalassinoides suevicus (Rieth 1932) (Fig. 9K)

Thalassinoides burrows are visible with Y-shaped branching on the lower bed surface. Burrows are elliptical to circular in cross section, 12–18 mm wide. *Thalassinoides* are assigned into groups of thalassinidean shrimp and part of callianassids mostly, which construct open burrow (Bromley 1996). A lot of fragments of *Thalassinoides* have been found at the L. Ondrašová locality.

Meandered sinusoidal trace fossils (Fig. 9L)

Width of burrow is 0.9 to 1.8 mm. Wavelength attains 13.4 mm and amplitude is 3.1 mm. This form of trace is rare and only one has been found on bedding sole at the Ráztoky locality. This type of trace can be attributed to fragments of meandered traces (e.g., *Protopaleodictyon*, *Belorhaphe*).

In addition to trace fossils and sole marks the rare body fossils were also found on the sandstone surfaces (Fig. 10A–D).

Calcareous nannofossils

All samples (for sample distribution see Fig. 3A) were positive and rich in calcareous nannofossils. Calcareous nannofossil preservation is moderate — mechanical damage, etching of the specimens is weak. The abundance of the calcareous nannofossils is moderate — about 10 specimens per field of view of the microscope.

The majority of the assemblage is composed of allochthonous species, Cretaceous and Eocene age.

Cretaceous species which were found: *Arkhangelskiella cymbiformis, Cyclagelosphaera reinhardtii, Chiastozygus* cf. *trabalis, Eiffelithus eximius, Lucianorhabdus* sp., *Micula* sp., *Zeugrhabdotus embergeri, Watznaueria barnesae, Watznaueria manivitae.*

Species that occur only in Eocene strata were found: *Discoaster barbadensis, Discoaster multiradiatus, Discoaster saipanensis, Chiasmolithus grandis, Neococcolithus dubius, Tribrachiatus contortus.*

A large part of the assemblage comprised species with their first occurrence in the Eocene and also they occur in Oligocene strata: *Chiasmolithus altus, Chiasmolithus oamaruensis, Cyclicargolithus floridanus, Dictyococcites bisectus, Discoaster nodifer, Helicosphaera bramlettei, Helicosphaera compacta, Isthmolithus recurvus, Lanternithus minutus, Pontosphaera latelliptica, Reticulofenestra hillae, Reticulofenestra moorei, Reticulofenestra umbilicus, Sphenolithus radians, Transversopontis pulcher* (Fig. 11).

Biostratigraphically significant species with their first occurrence in the Oligocene (see Fig. 11 and Table 2): *Cyclicargolithus abisectus, Helicosphaera recta, Reticulofenestra lockeri, Reticulofenestra ornata, Sphenolithus dissimilis*. They formed the smallest part of the nanno-assemblage.

On the basis of the detected nano-assemblage the Lower Oligocene age of the samples was determined. The NP23 Zone (Rupelian age) was determined by the species *Reticulofenestra lockeri, Reticulofenestra ornata, Helicosphaera recta, Sphenolithus dissimilis, Chiasmolithus altus, Transversopontis pulcher* and *Cyclicargolithus abisectus*.

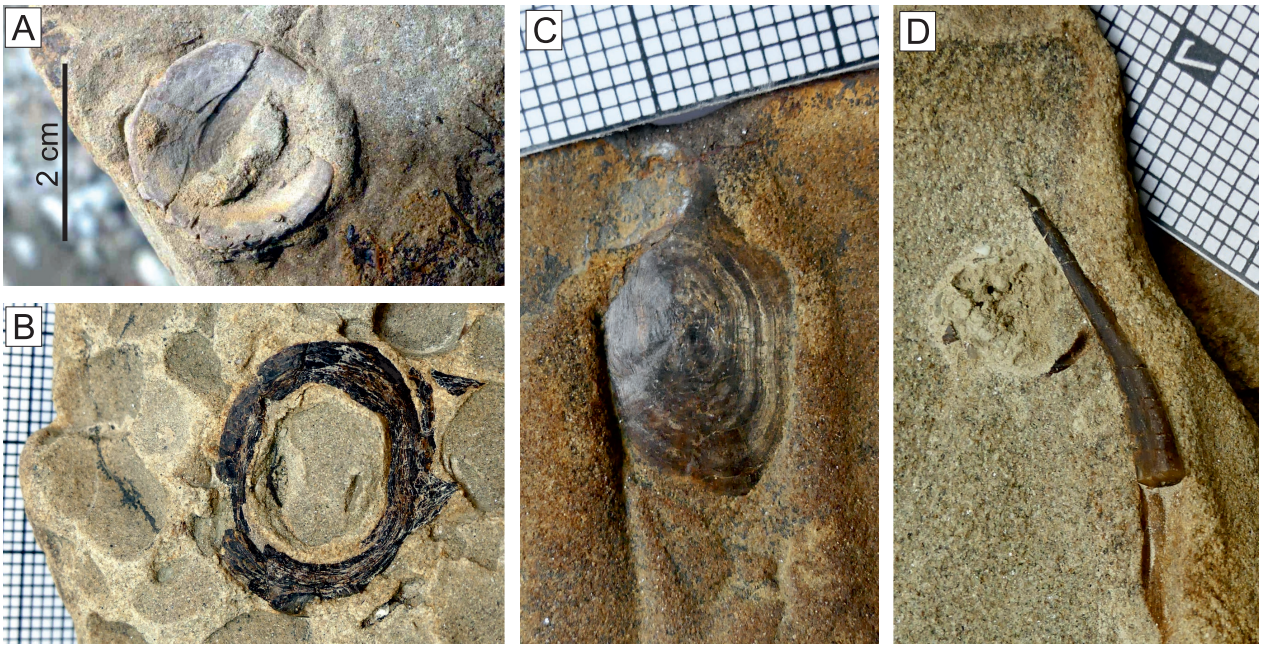

Fig. 10. Body fossils. **A** — Shark vertebra; **B** — circular fragment of a bone on the upper bed surface with shale rip-up clasts; **C** — fish scale; **D** — rib bone fragment; B–D scale in millimetres.

Cyclicargolithus abisectus was found only in the sample Lo-21 and first occurrence of this species is biostratigrafical significant for the NP23/24 Zone boundary (Perch-Nielsen 1985; Young 1998).

In six samples from non-profiled exposures (Ráztoky locality) *Isthmolithus recurvus* was indicated. It determines the lower part of the NP 23 Zone. The species *Isthmolithus recurvus* has the last occurrence in the Zone NP 23 (Perch-Nielsen 1985; Young 1998) (*see* Table 2).

Discussion

Most of the beds studied have the character of deposition from sandy high- to low density turbidity currents with typical vertical development of Bouma divisions. However, some beds show the repeated or symmetrical arrangement of individual facies within a single bed which should be caused by: hidden amalgamation in short successive turbidities or it is a reflection of waxing vs. waning processes in pulsating flows. The second case is more characteristic of turbulent hyperpycnal flows. However, frequent phytodetritic material as a characteristic diagnostic feature of hyperpycnites (if present in the source material, e.g., Zavala et al. 2012) was not observed here. Although the presence of phytodetritus was recorded in some sandstones (Fig. 5F) its occurrence is rather rare compared to other localities of the Zuberec Formation (cf. Starek & Fuksi 2017a,b; Kotulová et al. 2019).

The facies associations distinguished on the basis of the predominant sedimentary facies, sandstone bed thickness and proportion of mudstone facies have a close affinity to different components of distributive lobe deposits in a turbidity fan system. The mud-dominant zone (including the lowermost part of LO2) may correspond to the interlobe environment in the outer fan lobes but also may indicate either starvation of the basin or reduction of the sediment input to the basin's deeper part, probably related to relative sea-level rise (Johnson et al. 2001; Prélat et al. 2009; Grundvag et al. 2014). Frequent alternation of individual facies associations can be interpreted as a result of random shifting of lobe elements due to intrabasinal factors such as depositional topography (autogenic compensation processes), fan-channel switching, channel bifurcation and avulsion of channel or lobe shifting. On the basis of identified facies associations it is possible to interpret the sedimentary record of the studied outcrops as distal lobe deposits in an outer fan environment. This interpretation was also supported by the results of Hurst statistics which show that coarse division thickness and coarse division thickness percentage values define the environment as basin-floor sheet sand near the interface with lobe-interlobe deposits. Greater dissipation of values of the LO1 section located symmetrically around the border between basin-floor sheet sand and lobe interlobe deposits is caused by occurrence of a few thicker beds in the dataset. Coarse division thickness percentage represents harmonized data which minimize the effect of these thicker beds occurrence. The almost linear shape of cumulative distribution can also be correlated with the outer fan environment, not affected by significantly thicker amalgamated beds of the lobe axis and channels (Carlson & Grotziger 2001).

The identified trace fossils *Arthrophycus* cf. *tenuis*, *Scolicia strozzii*, *Strobilorhaphe clavata*, *Thalassinoides suevicus* from the Liptovská Ondrášová sections can be interpreted as a typical association for a turbidite depositional system of

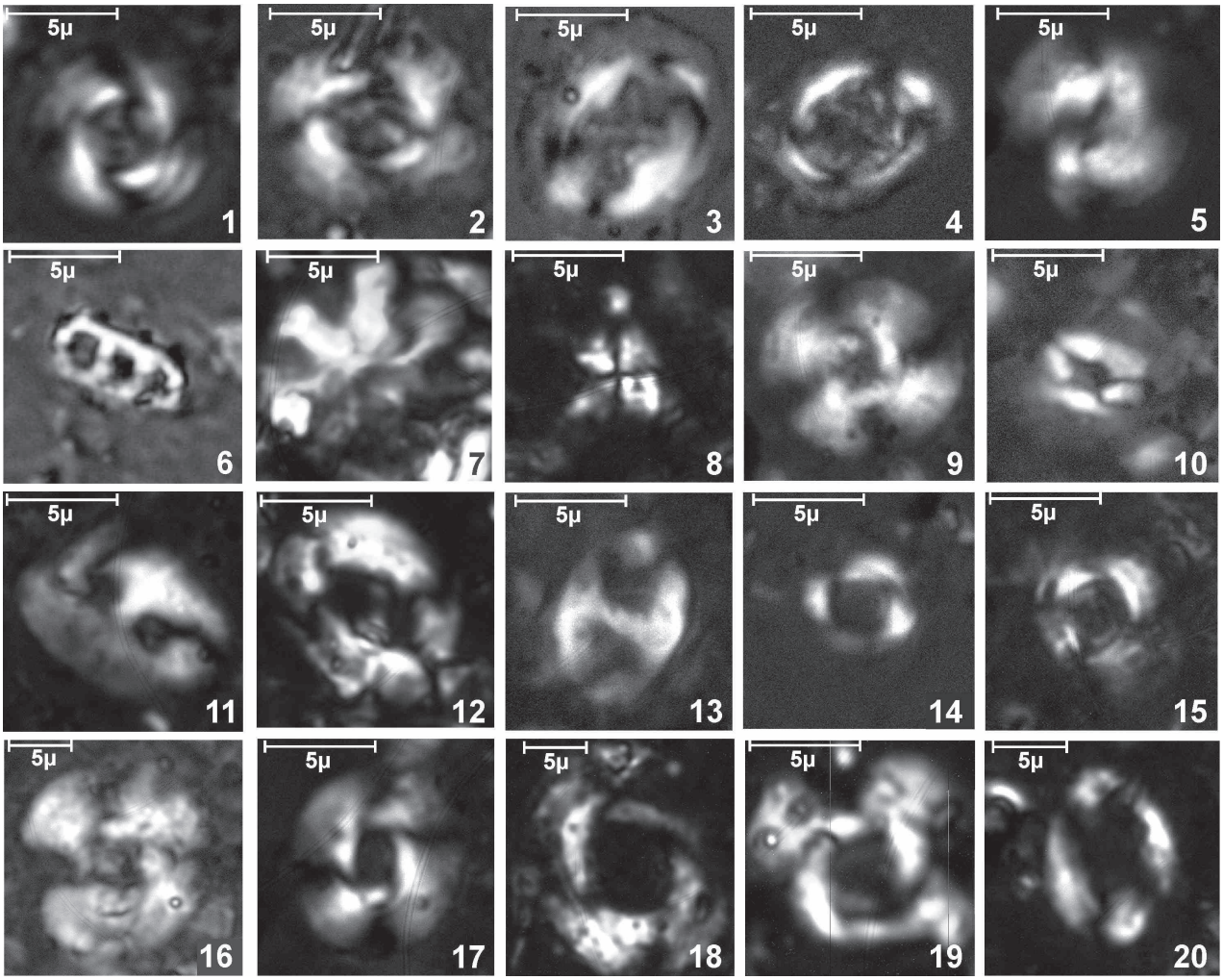

Fig. 11. Calcareous nannofossils from Liptovská Ondrašová and Ráztoky locations. **1, 2** — *Reticulofenestra lockeri*, samples: Lo-11, Lo-31; **3, 4** — *Chiasmolithus altus*, sample: Lo-21; **5** — *Dictyococcites bisectus* , sample: Lo-21; **6** — *Isthmolithus recurvus*, sample: Ráztoky 3; **7** — *Discoaster nodifer*, sample: Lo-14; **8** — *Sphenolithus dissimilis*, sample: Lo-12; **9** — *Cyclicargolithus floridanus*, sample: Lo-12; **10** — *Lanternithus minutus*, sample: Lo-21; **11** — *Helicosphaera recta*, sample: Lo-24; **12** — *Helicosphaera bramlettei*, sample: Lo-33; **13** — *Transversopontis pulcher*, sample: Lo-31; **14, 15** — *Reticulofenestra ornata*, samples: Lo-21, Lo-29; **16** — *Cyclicargolithus abisectus*, sample: Lo-15; **17** — *Reticulofenestra moorei*, sample: Lo-21; **18** — *Reticulofenestra umbilicus*, sample: Lo-21; **19** — *Reticulofenestra hillae*, sample: Lo-21; **20** — *Pontosphaera latelliptica*, sample: Lo-7.

archetypal *Cruziana* ichnofacies (Seilacher 1967; Knaust & Bromley 2012; MacEachern et al. 2007). This assemblage can be situated in the area of the turbidite sedimentary system of depositional lobes. Traces described within the Ráztoky locality section such as *Arenicolites* isp., *Bergaueria hemispherica*, *Saerichnites* isp. and questionable finds of *Paleodiction minimum*, fragments of sinusoidal graphoglyptids and *Laevicyclus* isp. present significant change of the ichnoassemblage. This change can be summarized as a change from an association of deposit feeders (e.g., *Helminthopsis tenuis*, *Planolites montanus*, *Scolicia strozzii*, *Thalassinoides suevicus*) to an association of shallow domichnia (*Arenicolites* isp., *Bergaueria hemispherica*, *Saerichnites* isp. that occupy the substrate to depths of 13–14 mm) and form traces of bottom surface association (*Paleodictyon minimum* and sinusoidal fragments of graphoglyptids). With regard to the thin layered lithology of the upper part of the studied section and occurrences of graphoglyptid fragments, this ichnoassemblage can be approximately compared with fan-fringe facies of *Paleodictyon–Nereites* subichnofacies (*sensu* Uchman 2007) with unusual association of *Arenicolites* isp., *Bergaueria hemispherica* and *Saerichnites* isp.

The predominantly thin-bedded development of turbidite sequences identified at the Liptovská Ondrášová and Ráztoky localities is characteristic rather for the facies association of the distal parts of the sandy fan. However, the available data from other parts of the CCPB point to a much greater variability of facies and facies associations within deposits of the Zuberec Formation (cf. Soták 1998; Starek & Fuksi 2017a,b). This variability can also be observed within the Liptov Depression itself. Especially in the middle to eastern part of the depression (in a wider area near settlements of

Table 2: Distribution of nannofossils in the Liptovská Ondrašová and Ráztoky outcrops with indications of important index species for biostratigraphic classification of the Oligocene formations.

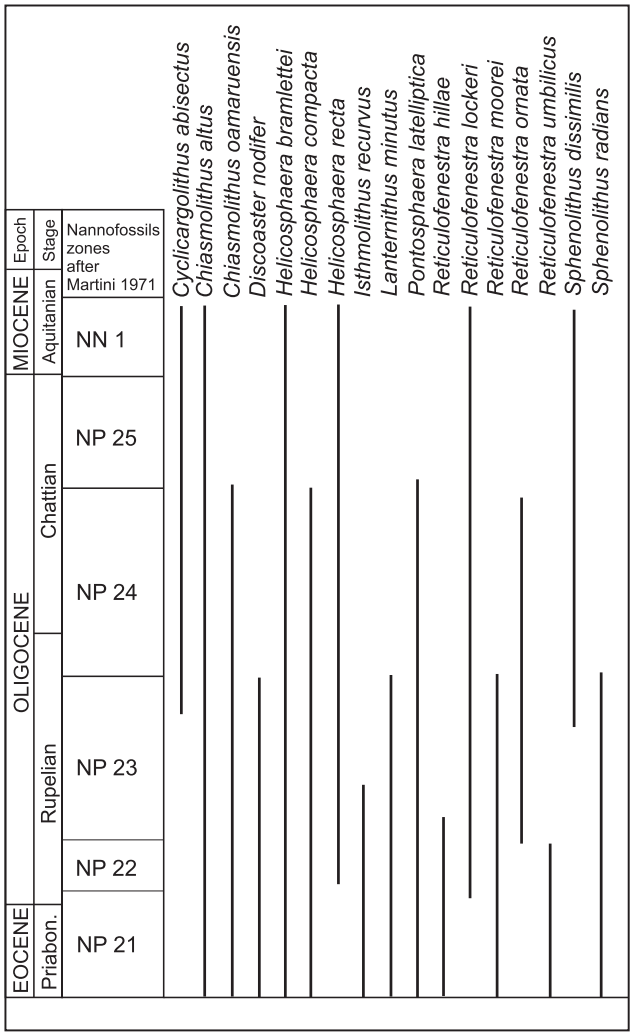

the Gôtovany, Bodice, Bobrovček, Bobrovec, Pavlová Ves, Liptovská Kokava and Liptovský Mikuláš town) there are tens of metres thick turbidity sequences with a slight mudstone predominance and similar sediment development to the outcrops studied. On the other hand, in other locations such as the Likavka–Ružomberok area and in the area of the Liptovská Mara Dam wall, the sequences of the Zuberec Formation have the character of medium- to thick-bedded turbidites with up to 1m thick massive sandstones (Gross et al. 1980). On the Liptovský Ondrej locality these turbidite sequences associate with the conglomerates of incised submarine slump. The variability of facies and facies associations within the Zuberec Formation is probably related to the position of the deposits studied within the depositional fan architecture and their spatial migration during the sequential-stratigraphic development of the CCPB.

The paleoecological evaluation of the nannofossil assemblage was done on the basis of autochthonous species. The majority of the autochthonous assemblage was formed by temperate-water species like *Cyclicargolithus, Reticulofenestra, Dictyococcites, Cocolithus*. Warm water species such as *Discoasters, Sphenolithus, Helicosphaera* are very rare. Cold water species such as *Reticulofenestra lockeri* and *Reticulofenestra ornata* also occurred in small numbers. *Reticulofenestra lockeri* and *Reticulofenestra ornata* are endemic species which tolerated hyposaline waters (Báldi-Béke 1984; Nagymarosy & Voronina 1992). This paleoecological condition is typical for the NP23/24 Zone (Báldi-Béke 1984; Nagymarosy 1990; Soták 2010).

Paleocurrent measurements point to the main transport of the material from SW and W which is generally consistent with the measurements of paleocurrents in the Orava–Podhale part of the CCPB (cf. Marschalko & Radomski 1960; Starek 2001; Starek & Fuksi 2017a). Uniform paleotransport mode suggests that the Liptov and Orava–Podhale sub-basins formed one sedimentary area without distinctive segmentation during the Oligocene. Rare opposite oriented paleocurrent indicators could be dimensions which occur in confined basins bounded by tectonic slopes or which would indicate feeding of depositional lobes from several sources. However, the scarcity of these results, as well as the fact that these paleocurrent data were derived from ripples, point rather to the combined flows and possible reworking of sandy fine-grained turbidites through bottom currents (e.g., Shanmungam et al. 1993; Martín-Chivelet et al. 2008).

Conclusions

The facies associations we have distinguished represent different components of distributive lobe deposits in a turbidite fan system. They correspond mainly to the lobe fringe and lobe distal fringe/inter-lobe facies associations with the local occurrence of medium bedded sequences corresponding to the lobe off-axis facies association. The interpretation as outer fan environment with basin-floor sheet sand near the interface with lobe–interlobe deposits was also supported by Hurst statistics and the shape of cumulative distribution. Relatively frequent alternation of individual facies associations within the evaluated sedimentary sections could be interpreted as a result of random shifting of depositional lobe elements and sedimentary facies.

An environment with turbidite deposition also generally corresponds to the identified trace fossil association of deep-tiering fodinichnia and domichnia up to shallow-tiering graphoglyptid traces.

The Rupelian age of the sedimentary sections near the Liptovská Ondrašová and Ráztoky localities was determined on the basis of the nanoassemblage detected.

Measurement of paleocurrents shows transport of material mainly from the SW and W. It is generally consistent with the paleotransport in Orava and Podhale, pointing to one sedimentation area without distinctive segmentation during the Oligocene.

Acknowledgements: This work was supported by the scientific grant agency of the Slovak Republic (Vega 2/0014/18) and Slovak Research and Development Agency under the contract No. APVV-14-0118. The authors are grateful to Ivana Koubová (Earth Science Institute of the SAS, Bratislava) for language correction. Thanks are also extended to Jozef Michalík (Earth Science Institute of the SAS, Bratislava), Alfred Uchman (Jagiellonian University, Kraków), Ľubomír Sliva (Nafta a.s., Bratislava) and an anonymous reviewer for the detailed review of the manuscript and constructive comments.

References

Arthur M.A., Dean W.E. & Stow D.A.V. 1984: Models for the deposition of Mesozoic–Cenozoic fine-grained organic–carbonrich sediment in the deep sea. In: Stow D.A.V. & Piper D.J.W. (Eds.): Fine-grained sediments: Deep-water processes and facies. *Geological Society of London Special Publications* 15, 527–560.

Báldi-Béke M. 1984: The nannoplankton of the Transdanubian Paleogene formations. *Geologica Hungarica, Series Paleontologica Institutum Geologicum Hungaricum Budapestini* 43, 1–223.

Baráth I. & Kováč M. 1995: Systematics of gravity-flow deposits in the marginal Paleogene formations between Markušovce and Kluknava villages (Hornád Depression). *Mineralia Slovaca, Geovestník* 27, 1–6 (in Slovak).

Baucon A., Ronchi A., Felletti F 2014: Evolution of crustaceans at the edge of the end-Permian crisis: ichnonetwork analysis of the fluvial succession of Nurra (Permian–Triassic, Sardinia, Italy). *Palaeogeogr. Palaeoclimatol. Palaeoecol.* 410, 74–103.

Biely A., Bezák V., Elečko M., Kaličiak M., Konečný V., Lexa J., Mello J., Nemčok J., Potfaj M., Rakús M., Vass D., Vozár J. & Vozárová A. 1996: Geological Map of Slovakia (1:500,000). *Geological Survey of Slovak Republic*, Bratislava.

Bouma A. H. 1962: Sedimentology of Some Flysch Deposits. *Elsevier*, Amsterdam, 1–168.

Bromley R.G. 1996: Trace Fossils. Biology, taphonomy and applications. Second edition. *Chapman & Hall*, 1–361.

Carlson J. & Grotzinger J.P. 2001: Submarine fan environment inferred from turbidite thickness distributions. *Sedimentology* 48, 1331–1351.

Chen Ch. & Hiscott R.N. 1999: Statistical analysis of facies clustering in submarine-fan turbidite successions. *J. Sediment. Res.* 69, 505–517.

Filipek A., Wysocka A & Barski M. 2017: Depositional setting of the Oligocene sequence of the Western Carpathians in the Polish Spisz region — a reinterpretation based on integ rated palynofacies and sedimentological analyses. *Geol. Quarterly* 61, 4, 859–876.

Fillion D. & Pickerill R.K. 1990: Ichnology of the Upper Cambrian? To Lower Ordovician Bell Island and Wabana groups of eastern Newfoundland, Canada. *Palaeontographica Canadiana* 7, 119.

Filo I. & Siráňová Z. 1996: The Tomášovce Member — a new lithostratigraphic unit of the Subtatric Group. *Geologicke Práce, Správy* 102, 41–49 (in Slovak with English summary).

Filo I. & Siráňová Z. 1998: Hornád and Chrasť Member — new regional lithostratigraphic units of the Sub-Tatric Group. *Geologické Práce, Správy* 103, 35–51 (in Slovak with English summary).

Fürsich F.T., Wilmsen M. & Seyed-Emami K. 2006: Ichnology of Lower Jurassic beach deposits in the Shemshak Formation at Shahmirzad, southeastern Alborz Mountains, Iran. *Facies* 52, 599–610.

Garecka M. 2005: Calcareous nannoplankton from the Podhale Flysch (Oligocene–Miocene, Inner Carpathians, Poland). In: Tyszka J., Oliwkiewicz-Miklasińska M., Gedl P. & Kaminski M.A. (Eds.): Methods and Applications in Micropalaeontology. *Studia Geologica Polonica* 124, 353–369.

Gedl P. 2000: Biostratigraphy and palaeoenvironment of the Podhale Palaeogene (Inner Carpathians, Poland) in the light of palynological studies. *Studia Geologica Polonica* 117, 155–303.

Geological map of Slovakia M 1:50,000 [online] 2013 [Geologická mapa Slovenska M 1:50 000]. *Štátny geologický ústav Dionýza Štúra*, Bratislava. http://apl.geology.sk/gm50js.

Gibert J.M. de & Goldring R. 2008: Spatangoid-produced ichnofabrics (Bateig Limestone, Miocene, Spain) and the preservation of spatangoid trace fossils. *Palaeogeogr. Palaeoclimatol. Palaeoecol.* 270, 299–310.

Golab J. 1959: On the geology of the western Podhale flysch area. *Biul. Inst. Geol.*, Warszawa, 1–149.

Gross P. 2008: Lithostratigraphy of Western Carpathians: Paleogene — Podtatranská Group. *Štátny Geologický Ústav D. Štúra*, Bratislava, 1–78 (in Slovak with English summary).

Gross P., Köhler E., Biely A., Franko O., Hanzel V., Hricko J., Kupčo G., Papšová J., Priechodská Z., Szalaiová V., Snopková P., Stránska M., Vaškovský I. & Zbořil Ľ. 1980: Geology of Liptovská kotlina depression [Geológia Liptovskej kotliny]. *Štátny Geologický Ústav D. Štúra*, Bratislava, 1–242 (in Slovak with English summary).

Gross P., Köhler E. & Samuel O. 1984: A new lithostratigraphic division of the Inner-Carpathian Paleogene. *Geologické Práce, Správy* 81, 113–117 (in Slovak with English summary).

Gross P., Köhler E., Mello J., Haško J., Halouzka R., Nagy A., Kováč P., Filo I., Havrila M., Maglay J., Salaj J., Franko O., Zakovič M., Pospíšil L., Bystrická H., Samuel O. & Snopková P. 1993: Geology of Southern and Eastern Orava [Geológia Južnej a Východnej Oravy]. *Geologický Ústav D. Štúra*, Bratislava, 1–319 (in Slovak).

Grundvag S.A., Johannessen E.P., Helland-Hansen W. & Plink-Björklund P. 2014: Depositional architecture and evolution of progradationally stacked lobe complexes in the Eocene Central Basin of Spitsbergen. *Sedimentology* 61, 535– 569.

Haq B.U. & Lohmann G.P. 1976: Early Cenozoic calcareous nannoplankton biogeography of the Atlantic Ocean. *Marine Micropaleontology* 1, 119–197.

Hurst H.E. 1951: Long-term storage capacity of reservoirs. *Transactions of the American Society of Civil Engineers* 116, 770–808.

Hurst H.E. 1956: Methods of using long-term storage in reservoirs. *Proceedings of the Institution of Civil Engineers* 5.5, 519–543.

Jach R., Gradzinski M. & Hercman H. 2016: New data on pre-Eocene karst in the Tatra Mountains, Central Carpathians, Poland. *Geol. Quarterly* 60, 2, 291–300.

Janočko J. & Jacko S. 1999: Marginal and deep-sea deposits of Central-Carpathian Paleogene Basin, Spiš Magura region, Slovakia: implication for basin history. *Slovak Geological Magazine* 4, 281–292.

Johnson S.D., Flint S.S., Hinds D. & Wickens H.D.V. 2001: Anatomy of basin floor to slope turbidite systems, Tanqua Karoo, South Africa: sedimentology, sequence stratigraphy and implications for subsurface prediction. *Sedimentology* 48, 987–1023.

Jopling A.V. & Walker R.G. 1968: Morphology and origin of ripple-drift cross-lamination, with examples from the Pleistocene of Massachusetts. *J. Sediment. Petrol.* 38, 971–984.

Kázmér M., Dunkl I., Frisch W., Kuhlemann J. & Ozsvárt P. 2003: The Palaeogene forearc basin of the Eastern Alps and Western Carpathians: subduction erosion and basin evolution. *J. Geol. Soc.* 160, 413–428.

Knaust D. & Bromley R. 2012: Trace Fossils as Indicators of Sedimentary Environments. *Developments in Sedimentology* 64, 1–924.

Kotulová J., Starek D., Havelcová M. & Pálková H. 2019: Amber and organic matter from the late Oligocene deep-water deposits of the Central Western Carpathians (Orava–Podhale Basin). *International Journal of Coal Geology* 207, 96–109.

Kováč M., Plašienka D., Soták J., Vojtko R., Oszczypko N., Less Gy., Ćosović V., Fügenschuh B. & Králiková S. 2016: Paleogene palaeogeography and basin evolution of the Western Carpathians, Northern Pannonian domain and adjoining areas. *Global Planet. Change* 140, 9–27.

Książkiewicz M. 1977: Trace fossils in the flysch of the Polish Carpathians. *Palaeontologia Polonica* 36, 1–208.

Kulka A. 1985: Arni sedimentological model in the Tatra Eocene. *Geol. Quarterly* 29, 31–64.

MacEachern J.A., Pemberton S.G., Gingras M.K. & Bann K.L. 2007: The ichnofacies paradigm: a fifty-year retrospective. In: Miller W., III, (Ed.): Trace Fossils. Concepts, Problems, Prospects. *Elsevier*, Amsterdam, 52–77.

Marshalko R. 1970: The research of sedimentary textures, structures, and palaeocurrent analysis of basal formations (Central Western Carpathian Paleogene, N of Spišsko-gemerské rudohorie Mts.). *Acta Geologica et Geographica Universitatis Comenianae* 19, 129–163.

Marschalko R. & Radomski A. 1960: Preliminary results of investigations of current directions in the fysch basin of the Central Carpathians. *Annales Societatis Geologurum Poloniae* 30, 3, 259–272.

Martini E. 1971: Standard Tertiary and Quaternary calcareous nannoplankton zonation. In: Proc. of the II. Planktonic Conference, Roma, 739–785.

Martín-Chivelet J., Fregenal-Martínez M.A. & Chacón B. 2008: Traction structures in contourites In: Rebesco M. & Camerlemghi A. (Eds.): Contourites. *Developments in Sedimentology* 60, 159–182.

Mulder T. & Alexander J. 2001: The physical character of subaqueous sedimentary density flows and their deposits. *Sedimentology* 48, 269–299.

Mutti E. 1992: Turbidite sandstones. *AGIP, Istituto di Geologia, Universita` di Parma*, 1–275.

Nagymarosy A. 1990: Paleogeographical and paleotectonical outlines of some intracarpathian Paleogene basins. *Geologický Zborník — Geologica Carpathica* 41, 3, 259–274.

Nagymarosy A. & Voronina A.A. 1992: Calcareous nannoplankton from the Lower Maykopian Beds (Early Oligocene, Union of Independent States). In: Harmšmid B. & Young J. (Eds.): Nannoplankton research. *Proc. 4th INA Conference, Prag, 1991, Knih. ZPN* 14b, 2, 189–221.

Olszewska B.W. & Wieczorek J. 1998: The Paleogene of the Podhale Basin (Polish Inner Carpathians) — micropaleontological perspective. *Przeglad Geologiczny* 46, 721–728.

Perch–Nielsen K. 1985: Cenozoic calcareous nannofossils. In: Bolli H., Saunders J.B. & Perch-Nielsen K.: Plankton stratigraphy. *Cambridge Univ. Press*, Cambridge, 427–554.

Pinheiro J., Bates D., DebRoy S., Sarkar D. & R Core Team 2018: nlme: Linear and Nonlinear Mixed Effects Models. R package version 3.1-137.

Piper D.J.W. 1978: Turbidite muds and silts on deep-sea fans and abyssal plains. In: Stanley D.J. & Kelling G. (Eds.): Sedimentation in submarine Canyons, fans and Trenches. *Dowden, Hutchinson and Ross*, Stroudsburg, 163–176.

Plašienka D. & Soták J. 2015: Evolution of Late Cretaceous–Palaeogene synorogenic basins in the Pieniny Klippen Belt and adjacent zones (Western Carpathians, Slovakia): tectonic controls over a growing orogenic wedge. *Annales Societatis Geologorum Poloniae* 85, 43–76.

Plička M. 1983: *Popradichnium erraticum* ichnogen. n. sp. n. — a new trace fossil from the Eocene Flysch of Slovakia. *Věstník Ústř. Ústavu geologického* 58, 5, 301–303.

Plička M. 1984: Two new fossil traces in Inner-Carpathian Paleogene in Slovakia (Czechoslovakia). *Západné Karpaty, sér. paleontológia*,9, 195–200.

Plička M. 1987: Fossil traces in the Inner-Carpathian Paleogene of Slovakia, Czechoslovakia. *Západné Karpaty, séria paleontológia* 12, 125–196.

Plička M., Němcová A. & Siráňová Z. 1990: Two new trace fossils in the Czechoslovak Carpathian Flysch — Result of the activity of Eel-like fish (Anquiliformes). *Západné Karpaty, séria paleontológia* 14, 109–123.

Prélat A., Hodgson D.M. & Flint S.S. 2009: Evolution, architecture and hierarchy of distributary deep-water deposits: a high-resolution outcrop investigation from the Permian Karoo Basin, South Africa. *Sedimentology* 56, 2132–2154.

Prélat A. & Hodgson D.M. 2013: The full range of turbidite bed thickness patterns in submarine lobes: controls and implications. *J. Geol. Soc.* 170, 209–2014.

Priestley M.B. 1981: Spectral Analysis and Time Series. *Academic Press*, London, New York, 1–890.

R Core Team 2014: R: A language and environment for statistical computing. *R Foundation for Statistical Computing*, Vienna, Austria. http://www.r-project.org/.

Rona P.A., Seilacher A., Vargas C., Gooday A.J., Bernhard J.M., Bowser S., Vetriani C., Wirsen C.O., Mullineaux L., Sherrell R., Grassle J.F., Lowh S. & Lutz R.A. 2009: *Paleodictyon nodosum*: A living fossil on the deep-seafloor. *Deep-Sea Research* II, 56, 1700–1712.

Roth P. H. & Thierstein H. 1972: Calcareous nannoplankton: leg. 14 of the Deep Sea Drilling Project. In: Hayes D.E., Pimm A.C., et al. (Eds.): *Initial reports DSDP* 14, 421– 485.

Samuel O. & Fusán O. 1992: Reconstruction of subsidence and sedimentation of Central Carpathian Paleogene. *Západné Karpaty, Séria Geológia*, 16, 7–46 (in Slovak with English summary).

Seilacher A. 1967: Bathymetry of trace fossils. *Mar. Geol.* 5, 413–428.

Seilacher A. 2007: Trace Fossil Analysis. *Springer*, Berlin, 1–226.

Shanmungam G., Spalding T.D. & Rofheart D.H. 1993: Process sedimentology and reservoir quality of deep-marine bottom-current reworked sands (sandy contourites): an example from the Gulf of Mexico. *AAPG Bull.* 77, 1241–1259.

Sliva Ľ. 2005: Sedimentary facies of the Central Carpathian Paleogene Basin from Spišská Magura. *PhD. Thesis, Department of Geology and Paleontology – Faculty of Natural Sciences CU*, Bratislava, 1–137 (in Slovak).

So Y.S., Rhee Ch.W., Choi P.-Y., Kee W.-S., Seo J.Y. & Lee E.-J. 2013: Distal turbidite fan/lobe succession of the Late Paleozoic Taean Formation, western Korea. *Geosciences Journal* 17, 1, 9–25.

Soták J. 1998: Sequence stratigraphy approach to the Central Carpathian Paleogene (Eastern Slovakia): eustasy and tectonics as controls of deep-sea fan deposition. *Slovak Geological Magazine* 4, 185–190.

Soták J. 2010: Paleoenvironmental changes across the Eocene–Oligocene boundary: insights from the Central-Carpathian Paleogene Basin. *Geol. Carpath.* 61, 5, 393–418.

Soták J., Pereszlenyi M., Marschalko R., Milička J. & Starek D. 2001: Sedimentology and hydrocarbon habitat of the submarine-fan deposits of the Central Carpathian Paleogene Basin (NE Slovakia). *Mar. Petrol. Geol.* 18, 87–114.

Soták J., Gedl P., Banská M. & Starek D. 2007: New stratigraphic data from the Paleogene formations of the Central Western Carpathians at the Orava region: Results of integrated micropaleontological study in the Pucov section. *Mineralia Slovaca* 39, 89–106 (in Slovak with English summary).

Starek D. 2001: Sedimentology and paleodynamic of Paleogene formations of the Central Westrn Carpathians in Orava. *PhD. Thesis, Geological Institute of the Slovak Academy of Sciences*, Bratislava, 1–152 (in Slovak with English summary).

Starek D. & Fuksi T. 2017a: Distal turbidite fan/lobe succession of the Late Oligocene Zuberec Fm. – architecture and hierarchy (Central Western Carpathians, Orava-Podhale basin). *Open Geosciences* 9, 1, 385–406.

Starek D. & Fuksi T. 2017b: Statistical analysis as a tool for identification of depositional palaeoenvironments in deep-sea fans (Palaeogene formations, Central Western Carpathians, north Slovakia). *Acta Geologica Slovaca* 9, 2, 2017, 149–162

Starek D., Andreyeva-Grigorovich A.S. & Soták J. 2000: Suprafan deposits of the Biely Potok Formation in the Orava region: Sedimentary facies and nannoplankton distribution. *Slovak Geological Magazine* 6, 188–190.

Starek D., Sliva L. & Vojtko R. 2004: The channel-levee sedimentary facies and their synsedimentary deformation: a case study from Huty Formation of the Podtatranská skupina Group (Western Carpathians). *Slovak Geological Magazine* 10, 177–182.

Starek D., Soták J., Jablonsky J. & Marschalko R. 2013: Large-volume gravity flow deposits in the Central Carpathian Paleogene Basin (Orava region, Slovakia): evidence for hyperpycnal river discharge in deep-sea fans. *Geol. Carpath.* 64, 305–326.

Stow D.A.V. & Shanmugam G. 1980: Sequence of structures in fine-grained turbidites: comparision of recent deep-sea and ancient flysch sediment. *Geology* 25, 23–42.

Stow D.A.V. & Piper D.J.W. 1984: Fine-grained sediments: Deepwater processes and facies. In: Stow D.A.V. & Piper D.J.W. (Eds.): *Geol. Soc. London, Spec. Publ.* 15, 1–659.

Šurka J., Sliva Ľ. & Soták J. 2012: Facial development of the Borové Formation in the area of Biely Potok at the town of Ružomberok and at Komjatná village (Western Carpathians, Slovakia). *Mineralia Slovaca* 44, 3, 267–278.

Uchman A. 1995: Taxonomy and palaeoecology of flysch trace fossils: The Marnoso-arenacea Formation and associated facies (Miocene, Northern Apennines, Italy). *Beringeria* 15, 1–115.

Uchman A. 1998: Taxonomy and ethology of flysch trace fossils: Revision of the Marian Książkiewicz collection and studies of complementary material. *Annales Societatis Geologorum Poloniae* 68, 105–218.

Uchman A. 2007: Deep Sea Ichnology: development of major concepts. In: W. Miller III (Ed.): Trace Fossils: Concepts, Problems, Prospects. *Elsevier*, 248–267.

Uchman A. & Rattazzi B. 2013: Scratch circles associatedwith the large foraminifer Bathysiphon from deep-sea turbiditic sediments of the Pagliaro Formation (Palaeocene), Northern Apennines, Italy. *Sediment. Geol.* 289, 115–123.

Westwalewicz-Mogilska E. 1986: A new look at the genesis of the Podhale Flysh. *Przegląd Geologiczny* 34, 690–698 (in Polish with English summary).

Wetzel A. & Bromley R.G. 1996: Re-evaluation of ichnogenus Helminthopsis Heer 1877 — a new look at the type material. *Palaeontology* 39, 1–19.

Wieczorek J. 1989: The Hecho model for Podhale flysh? *Przegląd Geologiczny* 37, 419–422 (in Polish).

Young J. R. 1998: Neogene. In: Bown P. R. (Ed.): Calcareous Nannofossil Biostratigraphy. *Kluwer Academic Publishers*, Dordrecht, 225–265.

Young, J.R., Bown P.R. & Lees J.A. 2017: Nannotax3 website. *International Nannoplankton Association*. http://www.mikrotax.org/Nannotax3.

Zavala C., Arcuri M., Di Meglio M., Gamero Diaz H. & Contreras C. 2011: A genetic facies tract for the analysis of sustained hyperpycnal flow deposits. In*:* R. M. Slatt & C. Zavala C. (Eds.): Sediment transfer from shelf to deep water — Revisiting the delivery system. *AAPG Studies in Geology* 61, 31–51.

Zavala C., Arcuri M. & Valiente L.B. 2012: The importance of plant remains as diagnostic criteria for the recognition of ancient hyperpycnites. *Revue de Paléobiologie* 11, 457–469.

Appendix

Checklist of taxa mentioned in the text in alphabetic order:

Nannoplankton species

Arkhangelskiella cymbiformis Vekshina, 1959
Chiasmolithus altus Bukry & Percival, 1971
Chiasmolithus grandis (Bramlette & Riedel, 1954) Radomski, 1968
Chiasmolithus oamaruensis (Deflandre, 1954) Hay et al., 1966
Cyclagelosphaera reinhardtii (Perch-Nielsen, 1968) Romein, 1977
Cyclicargolithus abisectus (Muller, 1970) Wise, 1973
Cyclicargolithus floridanus (Roth & Hay, in Hay et al., 1967) Bukry, 1971
Dictyococcites bisectus (Hay, Mohler, & Wade, 1966) Bukry & Percival, 1971
Discoaster barbadensis Tan, 1927
Discoaster nodifer (Bramlette & Riedel, 1954) Bukry, 1973
Discoaster multiradiatus Bramlette & Riedel, 1954
Discoaster saipanensis Bramlette & Riedel, 1954
Eiffelithus eximius (Stover, 1966) Perch-Nielsen, 1968
Helicosphaera bramlettei (Müller, 1970) Jafar & Martini, 1975
Helicosphaera compacta Bramlette & Wilcoxon, 1967
Helicosphaera recta (Haq, 1966) Jafar & Martini, 1975
Isthmolithus recurvus Deflandre in Deflandre & Fert, 1954
Lanternithus minutus Stradner, 1962
Neococcolithus dubius (Deflandre in Deflandre & Fert, 1954) Black, 1967
Pontosphaera latelliptica (Báldi-Beke & Baldi, 1974) Perch-Nielsen, 1974
Reticulofenestra hillae Bukry & Percival, 1971
Reticulofenestra lockeri Müller, 1970
Reticulofenestra moorei Bown & Dunkley Jones, 2012
Reticulofenestra ornata Müller, 1970
Reticulofenestra umbilicus (Levin, 1965) Martini & Ritzkowski,1968
Sphenolithus dissimilis Bukry & Percival, 1971
Sphenolithus radians Deflandre in Grassé, 1952
Transversopontis pulcher (Deflandre in Deflandre & Fert, 1954) Perch-Nielsen, 1967
Tribrachiatus contortus (Stradner, 1958) Bukry, 1972
Zeugrhabdotus embergeri (Noël 1959) Perch-Nielsen, 1984
Watznaueria barnesae (Black in Black & Barnes, 1959) Perch-Nielsen, 1968
Watznaueria manivitae Bukry, 1973